Probing Selectivity over Pt−Sn Catalysts in Reactions of *n*-C_6 Hydrocarbons: Adsorption and Reactivity of *n*-Hexane, 1-Hexene, and 1,5-Hexadiene on Pt(111) and Sn/Pt(111) Surface Alloys

Haibo Zhao and Bruce E. Koel*,†

Department of Chemistry, and Center for Advanced Materials and Nanotechnology (CAMN), Lehigh University, Bethlehem, Pennsylvania 18015-3128

Received: April 4, 2009; Revised Manuscript Received: August 17, 2009

We have investigated how alloyed Sn at a Pt(111) surface alters the adsorption, desorption, and reactive chemistry of linear C_6-hydrocarbon molecules containing an increasing degree of unsaturation: *n*-hexane, 1-hexene, and 1,5-hexadiene. This chemistry was investigated on Pt(111) and two bimetallic surfaces, the (2 × 2)-Sn/Pt(111) and ($\sqrt{3} \times \sqrt{3}$)R30°-Sn/Pt(111) surface alloys, by using temperature-programmed desorption and Auger electron spectroscopy. *n*-Hexane weakly and reversibly adsorbed on all three surfaces, but 1-hexene and 1,5-hexadiene chemisorbed and underwent dehydrogenation depending on the surface. Increasing the Sn concentration decreased the adsorption energy of all three molecules, but the effect was most pronounced for the unsaturated hydrocarbons upon changing from the (2 × 2) alloy to the ($\sqrt{3} \times \sqrt{3}$)R30° alloy. All three molecules only weakly and reversibly adsorb and have nearly the same adsorption energies, on a thick Sn film. Alloying with Sn decreased the amount of irreversibly chemisorbed 1-hexene at monolayer coverage from 65% on Pt(111) to 18% on the (2 × 2) alloy, and dehydrogenation was eliminated on the ($\sqrt{3} \times \sqrt{3}$)R30° alloy. Similarly, alloying with Sn decreased irreversible 1,5-hexadiene chemisorption at monolayer coverage from 100% on Pt(111) to 30% on the (2 × 2) alloy, and dehydrogenation was completely eliminated on the ($\sqrt{3} \times \sqrt{3}$)R30° alloy. Reversible alkene and diene adsorption is associated with the elimination of pure-Pt 3-fold sites on the ($\sqrt{3} \times \sqrt{3}$)R30° alloy. Furthermore, the amount of 1-hexene dehydrogenation was linearly related to the number of pure-Pt 3-fold sites on these three surfaces. Alloying Sn with Pt(111) did not decrease the saturation monolayer coverage of any of the three molecules. This work extends our understanding of hydrocarbon chemistry at Pt−Sn alloy surfaces and may aid in understanding current catalysts used for hydrocarbon reforming and the development of new catalysts for selective hydrogenation.

1. Introduction

Supported platinum catalysts are widely used to carry out skeletal reactions of alkanes, an important process in naphtha reforming. The mechanism of forming cyclic molecules from hexane has long been a matter of dispute.[1−4] "Direct" and "hexatriene" pathways for benzene formation have been proposed over supported Pt.[5] Hexenes,[6] hexadienes,[7] and hexatriene[8] from stepwise dehydrocyclization of hexane on Pt black have been observed as reaction intermediates, even in the presence of excess hydrogen.[9]

Addition of catalytically inactive Sn has been considered to dilute contiguous Pt sites at the bimetallic surface to create smaller ensembles favorable for nondegradative reactions and decreasing the C−H and C−C bond breaking activity of Pt in catalysts used for reforming reactions. Sn modification of the catalytic properties of Pt has been investigated by many researchers.[10−16] In particular, Llorca et al.[17] studied selective dehydrogenation of 1-hexane on supported Sn−Pt catalysts. They found that increasing the Sn concentration greatly increased the selectivity to form 1-hexene and reduced the selectivity to produce benzene. They proposed that the selectivity for a particular dehydrogenated product was related to both ensemble (or geometric) and electronic (or ligand) effects, and the decrease in benzene selectivity was due to the facile desorption of olefins when Sn was added to the catalyst. Dautzenberg et al.[15] and Biloen et al.[18] suggested that the effect of Sn was to divide the surface into a smaller number of contiguous Pt atoms, and this arrangement brought about beneficial effects on the selectivity and stability of the catalyst (an ensemble effect). However, Burch and Garla[11] proposed that the role of Sn was to modify the electronic properties of the small platinum particles (a ligand effect).

A molecular level understanding of the origin of the beneficial effects observed for commercial bimetallic supported catalysts is very difficult because a multitude of different phases can exist, and even many types of bimetallic structural features can occur such as bimetallic clusters, alloys, metal−particle edge decoration, and reconstructed crystalline facets. Two well-characterized, ordered Sn/Pt(111) surface alloys, first reported by Paffett and Windham,[19] offer outstanding new opportunities for fundamental surface science and catalytic studies at the molecular level. We have used these surfaces to probe the influence of alloyed Sn at a Pt(111) surface in comparative studies of *n*-hexane, 1-hexene, and 1,5-hexadiene adsorption and reaction. Adsorption on a thick Sn film was also investigated in order to provide additional benchmark information to help understand the surface chemistry on these alloys.

Only three surface science studies of the adsorption of these three molecules on Pt(111) or Sn/Pt alloys have been reported. Reflection−absorption infrared spectroscopy (RAIRS) spectra

* Corresponding author. Phone: 1-610-758-6120. E-mail: brk205@lehigh.edu.
† Current address: Huntsman Advanced Technology Center 8600 Gosling Road The Woodlands, Texas 77381.

10.1021/jp903127b CCC: $40.75
Published on Web 09/25/2009

after *n*-hexane adsorption on Pt(111) showed that the carbon chain is almost exclusively parallel to the metal surface at monolayer coverage.[20] The desorption activation energy, E_d, reported by Nuzzo et al. by using TPD was 12.8 kcal/mol.[21] RAIRS studies of 1-hexene decomposition on Pt(111) showed that chemisorbed 1-hexene starts to decompose at 250 K by forming hexylidyne ($\equiv C(CH_2)_4CH_3$).[22] In related studies, butane is reversibly adsorbed on Pt(111),[23] but cyclohexane partially decomposes on Pt(111) during heating in TPD.[24] Adsorption and reaction studies of ethylene,[25] propene,[26] and 1-butene[27] on Pt(111) and these two Sn/Pt(111) surface alloys have shown that the substantial fraction of decomposition of these three alkenes on Pt(111) is greatly suppressed by alloying Sn in Pt(111). All of these three alkenes reversibly adsorb on the ($\sqrt{3} \times \sqrt{3}$)R30°-Sn/Pt(111) surface alloy. No decomposition occurs during heating in TPD because the molecular desorption activation energies are lower than the corresponding C−H bond breaking barriers on this surface. Compared with 1-butene, 1-hexene and 1,5-hexadiene are longer chain hydrocarbons (by two carbons), and 1,5-hexadiene has an additional C=C double bond. This will cause an increase in the adsorption energies, which may be sufficient on the Sn/Pt(111) alloy surfaces to open up decomposition pathways and probe C−H bond breaking barriers. Another pathway, cyclization, may also occur for 1,5-hexadiene since cyclohexadiene has been observed to form high yields of benzene on these alloy surfaces.[28]

2. Experimental Methods

Experiments were performed in a three-level UHV chamber that has been described earlier.[29] The Pt(111) crystal (Atomergic; 10 mm diam, 1.5 mm thick) was prepared by 1 keV Ar^+-ion sputtering and oxygen treatments (5×10^{-7} torr O_2, 900 K, 2 min) to give a clean spectrum using Auger electron spectroscopy (AES) and a sharp (1 × 1) pattern in low energy electron diffraction (LEED).

The (2 × 2)-Sn/Pt(111) and ($\sqrt{3} \times \sqrt{3}$)R30°-Sn/Pt(111) surface alloys were prepared by evaporating about two monolayers of Sn onto the Pt(111) crystal surface and subsequently annealing the sample to 1000 and 830 K for 30 s, respectively. On surfaces prepared as above, Sn is incorporated substitutionally into the surface layer at Pt lattice sites to form an ordered surface alloy with $\theta_{Sn} = 0.25$, corresponding to the (111) face of Pt_3Sn, and $\theta_{Sn} = 0.33$, corresponding to a Pt_2Sn surface structure. Sn atoms are "buckled" outward and protrude 0.02 nm above the surface−Pt plane on both surfaces.[30] For the (2 × 2) structure, pure-Pt 3-fold sites are present, but no adjacent pure-Pt 3-fold sites exist. All pure-Pt 3-fold sites are eliminated in the ($\sqrt{3} \times \sqrt{3}$)R30° structure. For brevity throughout this paper, we will refer to the (2 × 2)-Sn/Pt(111) and ($\sqrt{3} \times \sqrt{3}$)R30°-Sn/Pt(111) surface alloys as the (2 × 2) and $\sqrt{3}$ alloys respectively. Also, we evaporated Sn onto the Pt(111) surface until the Pt peak was no longer detected in AES to form a thick Sn film, and we investigated adsorption on this film too.

n-Hexane (Mallinckrodt, AR), 1-hexene (Aldrich Chemical Co., 97%), and 1,5-hexadiene (Alfa Aesar, 98%) were placed in glass reservoirs attached to a stainless steel dosing line and used as supplied after degassing by multiple freeze−pump−thaw cycles. These molecules were exposed on the Pt crystal by a microcapillary array doser connected to the gas line via a leak valve. All of the exposures reported herein are given simply in terms of the pressure measured by the ion gauge. No attempt was made to correct for the flux enhancement of the doser or ion gauge sensitivity. The mass spectrometer in the chamber was used to check the purity of the gases during dosing.

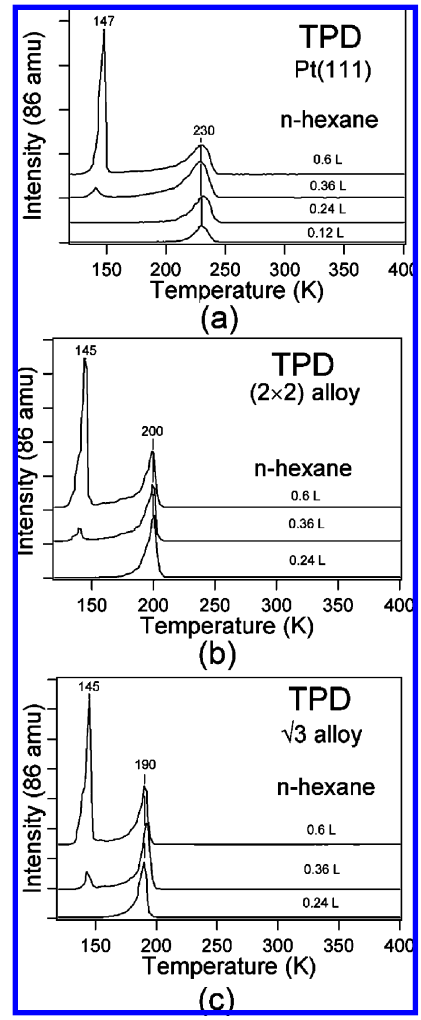

Figure 1. *n*-hexane (C_6H_{14}) TPD traces following *n*-hexane exposures on (a) Pt(111) and the (b) (2 × 2)-Sn/Pt(111) and (c) ($\sqrt{3} \times \sqrt{3}$)R30°-Sn/Pt(111) alloys at 110 K.

The heating rate was 3.6 K/s for all TPD experiments, and all exposures were given with the surface temperature at 110 K. AES measurements were made with a double-pass cylindrical mirror analyzer (CMA). The electron gun was operated at 3 keV beam energy and 1.5 μA beam current. Coverages, θ, reported in this paper are referenced to the surface atom density of Pt(111) such that θ_{Pt} =1.0 ML is defined as 1.505×10^{15} atoms cm^{-2}.

3. Results

3.1. *n*-Hexane, C_6H_{14}. TPD spectra showing *n*-hexane (C_6H_{14}) desorption from Pt(111) and the (2 × 2) and $\sqrt{3}$ alloys are shown in Figure 1, respectively. After low exposures, a desorption peak at 230 K from chemisorbed *n*-hexane was observed. Physisorbed species in the second layer formed after larger *n*-hexane exposures desorbed in low-temperature peaks near 145 K on all three surfaces. Our results are consistent with those observed by Nuzzo and co-workers,[21] although the monolayer peak in Figure 1 was 9 K lower than they observed. Alloying Sn with Pt(111) decreased the temperature of *n*-hexane desorption from the monolayer on the (2 × 2) and $\sqrt{3}$ alloys, forming peaks at 200 and 190 K, respectively. Analysis of these desorption peak temperatures leads to desorption activation energies of E_d = 59, 51, and 48 kJ/mol, respectively, by using the Redhead approach and assuming a pre-exponential factor of 1×10^{13} s^{-1} and first order desorption kinetics.[31]

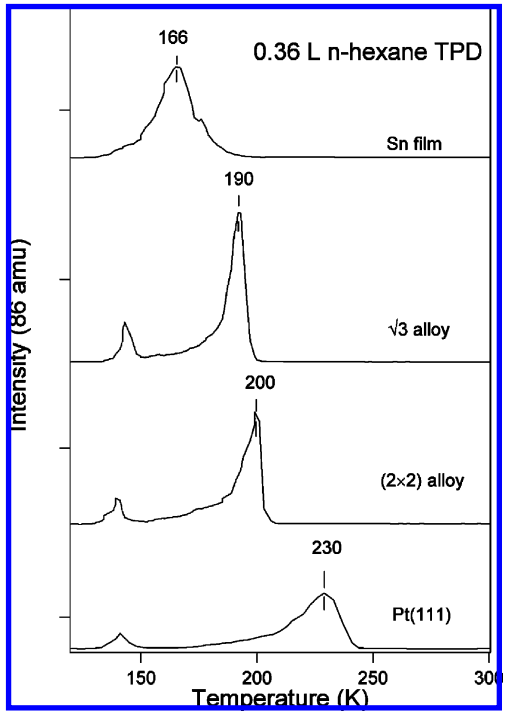

Figure 2. Comparison of the *n*-hexane (C_6H_{14}) TPD curves after 0.36-L *n*-hexane exposures that produce coverages near one monolayer on Pt(111), the (2 × 2)-Sn/Pt(111) and ($\sqrt{3} \times \sqrt{3}$)R30°-Sn/Pt(111) alloys, and a thick Sn film at 110 K.

No other desorbed products from reaction or decomposition were detected upon heating in TPD experiments (signals at 86, 84, 82, 80, 78, 28, 18, and 2 amu were monitored during TPD). In particular, H_2 evolution from *n*-hexane dehydrogenation on Pt(111) and the Sn/Pt(111) alloys was negligible. Consistent with these TPD results, no carbon was detected by AES following any of the TPD experiments.

Figure 2 compares molecular *n*-hexane desorption spectra from Pt(111), the two Sn/Pt(111) alloys, and a thick Sn film, for a coverage close to saturating the monolayer on each surface. The desorption peak temperature shifted down as the surface Sn concentration increased. *n*-Hexane desorbs on these Sn/Pt(111) alloys in a single, relatively narrow desorption peak, which implies that there is a single, well-defined adsorption energy for *n*-hexane on these bimetallic surfaces that is characteristic of each alloy. This behavior was also observed for butane desorption from these alloy surfaces.[23] *n*-Hexane only weakly adsorbs on pure Sn, and the monolayer desorption peak from a thick Sn film occurs at 166 K. This peak is only 20 K higher than the desorption peaks on Pt(111) and Pt(111)/Sn alloys, as in Figure 1, from condensed *n*-hexane two-layer films. This shows the expected result that the interaction between *n*-hexane and the Sn surface is weak but slightly stronger than the intermolecular interactions between *n*-hexane molecules in the condensed phase.

The coverage of *n*-hexane in the monolayer on Pt(111) can be determined by measuring the peak-to-peak ratio of C (272 eV) and Pt (237 eV) signals in AES obtained from the *n*-hexane monolayer. This was produced by annealing the sample to 160 K for 5 s after a 0.36 L exposure of *n*-hexane. This C(272)/Pt(237) AES ratio was then compared to that obtained following a saturation exposure of ethylene (C_2H_4) on Pt(111) at 300 K, which produces 0.25 ML ethylidyne (CCH_3).[32] The relative sizes of these signals give the relative coverage of *n*-hexane, assuming that the C(272)/Pt(237) AES ratio is linear in carbon coverage

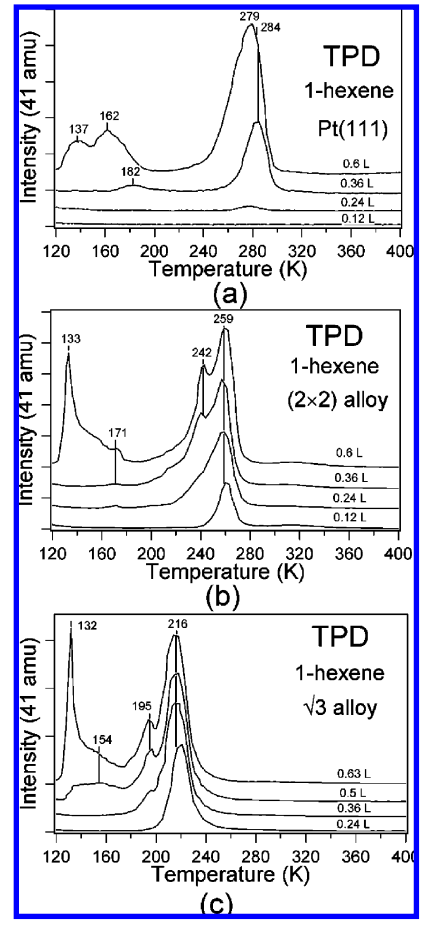

Figure 3. 1-Hexene (C_6H_{12}) TPD traces following 1-hexene exposures on (a) Pt(111) and the (b) (2 × 2)-Sn/Pt(111) and (c) ($\sqrt{3} \times \sqrt{3}$)R30°-Sn/Pt(111) alloys at 110 K.

over the small range of coverages involved. Then the relative coverage of *n*-hexane in the monolayers on the two Sn/Pt alloys in comparison to Pt(111) can be derived readily from the relative TPD peak areas. The *n*-hexane monolayer coverages on Pt(111) and the (2 × 2) and $\sqrt{3}$ alloys were 0.23, 0.24, and 0.25 ML, respectively. The larger apparent monolayer coverage of 0.31 ML on the Sn film may be caused by surface roughness in the film due to nonideal layering in the film, which was grown at low temperature, and this could also contribute to the breadth of the desorption peak.

3.2. 1-Hexene, C_6H_{12}. Figure 3a shows a series of 1-hexene (C_6H_{12}) TPD spectra obtained by monitoring the major cracking fraction (41 amu) signal of 1-hexene in the QMS after 1-hexene adsorption on Pt(111) at 110 K. Other than molecular 1-hexene, and H_2 from 1-hexene dehydrogenation, no other desorbed reaction products were detected in our TPD experiments. Signals at 86, 84, 82, 80, 78, 28, 18, and 2 amu were monitored. For small exposures, 1-hexene is irreversibly adsorbed and no molecular desorption occurs during subsequent heating in TPD. Chemisorbed 1-hexene initially desorbs in a peak at 284 K, with E_d = 73 kJ/mol. The slight peak shift to 279 K when the monolayer saturation coverage is reached is likely caused by weak lateral repulsive interactions in the monolayer. Further exposures resulted in low temperature peaks and eventually populated some weakly bonded species characteristic of multilayer desorption.

Figure 3b shows TPD spectra of 1-hexene desorption after increasing exposures of 1-hexene on the (2 × 2) alloy at 110 K. After small exposures, molecular 1-hexene desorption was

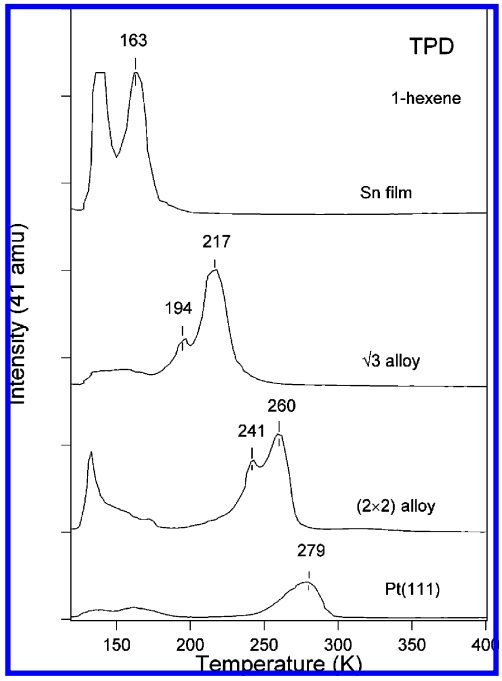

Figure 4. Comparison of the 1-hexene (C_6H_{12}) TPD curves after 1-hexene exposures that produce coverages near one monolayer on Pt(111), the (2 × 2)-Sn/Pt(111) and ($\sqrt{3} \times \sqrt{3}$)R30°-Sn/Pt(111) alloys, and a thick Sn film at 110 K.

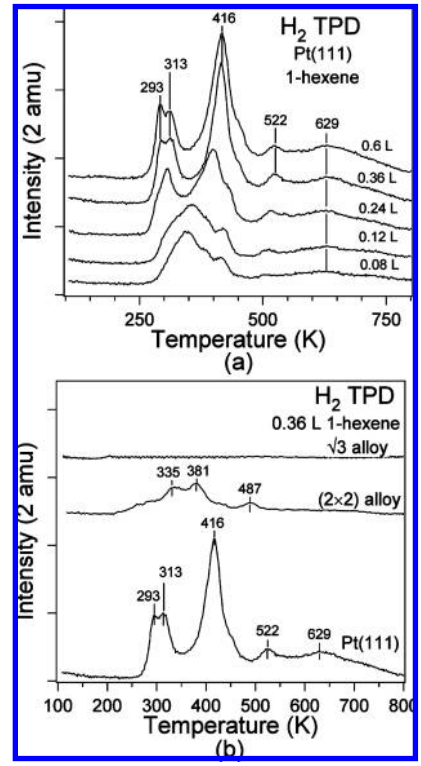

Figure 5. (a) H_2 TPD traces resulting from 1-hexene dehydrogenation after 1-hexene exposures on Pt(111) at 110 K. (b) Comparison of the H_2 TPD curves after 0.36-L 1-hexene exposures that produce coverages near one monolayer on Pt(111) and the (2 × 2)-Sn/Pt(111) and ($\sqrt{3} \times \sqrt{3}$)R30°-Sn/Pt(111) alloys at 110 K.

observed in a peak at 259 K ($E_d = 66$ kJ/mol). A new desorption peak at 242 K ($E_d = 62$ kJ/mol) was observed after an exposure of 0.36 L, also due to desorption from the chemisorbed layer. A low-temperature peak at 133 K could be increased in size without limit using larger exposures and thus is attributed to desorption from physisorbed multilayer states.

A series of 1-hexene TPD spectra following increasing 1-hexene exposures on the $\sqrt{3}$ alloy is shown in Figure 3c. After small exposures, a single desorption peak at 216 K ($E_d = 55$ kJ/mol) was observed, but a second desorption peak at 195 K ($E_d = 49$ kJ/mol) is also assigned to desorption from the monolayer. At a coverage prior to the formation of the sharp multilayer peak at 132 K, another broad desorption feature appeared near 154 K.

Figure 4 compares TPD curves for 1-hexene molecular desorption from Pt(111), two Sn/Pt(111) surface alloys, and a thick Sn film. This shows more clearly how the desorption peak temperature of 1-hexene in the monolayer shifts down as the surface Sn concentration increases. The 163 K peak on the Sn film is very close to that for *n*-hexane in Figure 2, consistent with a weak physisorption interaction. On Pt(111), the amount of molecular 1-hexene desorption is smaller than that from the two alloys even though similar monolayer coverages were formed (as discussed below). This is due to the greater extent of decomposition that occurs on Pt(111) compared with that on the alloys during TPD, as shown more clearly by the H_2 TPD spectra shown in Figure 5. Thus, alloyed Sn weakens the bonding of 1-hexene to the Pt(111) surface and suppresses the decomposition of chemisorbed 1-hexene. Unlike 1-hexane, the amount of 1-hexene desorption from the adsorbed monolayer on a thick Sn film was less than that from the two surface alloys. This may be caused by surface roughness (nonideal layering) in the film, which can vary with the preparation of each film.

Small (C_2-C_5) linear alkenes are all di-σ-bonded to Pt(111) at 100−230 K,[33−35] and 1-hexene has a desorption activation energy that is similar to that for ethylene,[25] propene,[26] and 1-butene.[27] It is reasonable to infer that 1-hexene is also di-σ-bonded on Pt(111). Chesters and co-workers[22] concluded that this species was converted to adsorbed hexylidyne ($(\equiv C(CH_2)_4CH_3)$ at 250 K. We found previously[25] that ethylene was still di-σ-bonded on both of these alloys but that it was less rehybridized from sp^2 toward sp^3 as the alloyed Sn concentration increased. Observation of similar decreases in the desorption activation energy, that is, weakening of the chemisorption bond strength, for 1-hexene and ethylene suggests that di-σ-bonded 1-hexene is also present on the surfaces of these two alloys at low temperature.

We have no clear assignment of the origin of the weakly bonded states that desorb from Pt(111) and two Sn/Pt alloy surfaces at 150−180 K. Similar features were also observed for 1-butene and isobutene[27] adsorption on the two surface alloys. We suppose that these states are not really part of the chemisorbed monolayer; that is, they do not have site-specific and geometry-specific bonding interactions with the surface, but they do have a fair energetic distinction from other physisorbed, second-layer and multilayer species on these surfaces due to some appreciable additional interaction with the surface.

H_2 TPD spectra following various exposures of 1-hexene on Pt(111) at 110 K are shown in Figure 5a. The H_2 yield was constant for all exposures larger than 0.6 L. Below this value, the H_2 yield increased with increased 1-hexene exposure even though molecular 1-hexene desorption starts at an exposure near 0.24 L, as shown in Figure 3. This competition between dehydrogenation and molecular desorption is different from that observed in 1-butene TPD on Pt(111),[27] where the H_2 yield saturated as soon as molecular 1-butene desorption began. After 1-hexene exposures of 0.12 L or below, H_2 desorption occurred primarily in a broad feature peaked at 348 K with a shoulder at

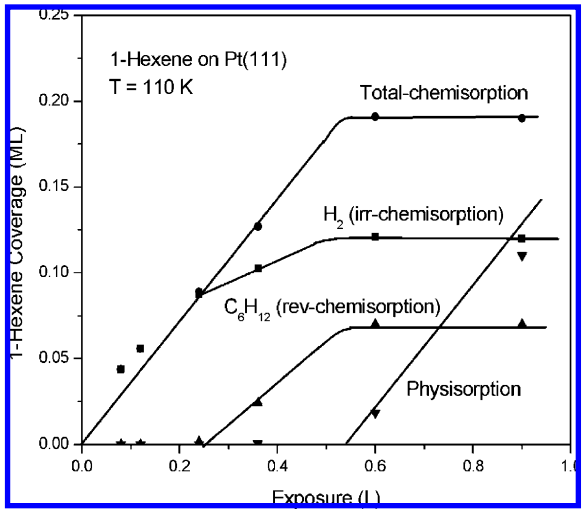

Figure 6. Uptake curves showing adsorption kinetics as derived from TPD experiments for 1-hexene adsorption on Pt(111) at 110 K. Total chemisorption: the amount of 1-hexene that chemisorbs at 110 K. H_2 (irr-chemisorption): the amount of 1-hexene dehydrogenating in TPD that is calculated from H_2 TPD peak areas. C_6H_{12} (rev-chemisorption): the amount of chemisorbed 1-hexene that desorbs as 1-hexene in TPD. Physisorption: the amount of physisorbed 1-hexene that desorbs in TPD in peaks at very low temperature.

422 K. This is similar to that observed for 1-butene on Pt(111). Some weak H_2 desorption features also extend from 500−800 K. H_2 desorption after H_2 exposures occurs about 350 K, and this indicates that the lowest temperature H_2 evolution from dehydrogenation of low coverages of 1-hexene is likely to be H_2-desorption rate-limited. Previous RAIRS results[22] identified that 1-hexene dehydrogenated to form hexylidyne at 270 K. The H_2 desorption profile from the 1-hexene monolayer on Pt(111) has a characteristic structure with six identifiable peaks or features at 293, 313, 416, 450, 522, and 629 K.

H_2 desorption spectra from 1-hexene monolayers on Pt(111) and the (2 × 2) and $\sqrt{3}$ alloys are compared in Figure 5b. The amount of H_2 evolved from the (2 × 2) alloy is only 27% of the H_2 yield from Pt(111). This corresponds to dehydrogenation of 18% of the chemisorbed 1-hexene monolayer on the (2 × 2) alloy (as determined below). No H_2 desorption was detected from the $\sqrt{3}$ alloy because of 1-hexene reactions. Thus, alloying Sn dramatically suppressed the surface reactivity and the amount of 1-hexene dehydrogenation (as monitored by the H_2 desorption yield) on both alloys. AES measurements taken after TPD experiments on both alloys were fully consistent with these conclusions based on the H_2 TPD results.

Figure 6 summarizes the adsorption kinetics of 1-hexene on Pt(111) at 110 K obtained from TPD measurements. This "uptake curve" also provides information on the monolayer saturation coverage and amount of 1-hexene dehydrogenation during TPD. H_2 and C_6H_{12} were the only gases observed to desorb from the surface, and these product yields reflect the amounts of reversible and irreversible chemisorption. Calibration of such an uptake curve is reported in more detail elsewhere.[26] Briefly, we utilized the H_2 TPD yield from the well-known dehydrogenation of 0.25 ML ethylidyne (CCH_3) on Pt(111) to give an absolute calibration for the H_2 TPD area from irreversibly adsorbed 1-hexene. Assuming the sticking coefficient of 1-hexene on Pt(111) at 110 K is independent of coverage, we can then calibrate the 1-hexene TPD area by forcing the slope of the total 1-hexene uptake curve to be same as that for the irreversibly adsorbed curve before molecular 1-hexene desorption occurs. The monolayer saturation coverage of chemisorbed 1-hexene is given by the sum of the two curves, irreversibly and reversibly adsorbed 1-hexene. In this manner, we determine that this value was 0.19 ML on Pt(111) and 65% of the monolayer fully dehydrogenated during TPD. This approach provides a relationship between 1-hexene desorption peak area and 1-hexene coverage, and this was used to calibrate the 1-hexene saturation coverage on the two alloys, which was 0.18 and 0.20 ML on (2 × 2) and $\sqrt{3}$ alloys, respectively.

The above method requires a significant region in which all chemisorbed molecules are irreversibly adsorbed and there is no competition between molecular desorption and dehydrogenation. If such a situation is not realized, one can use a second method to estimate the saturation coverage and dehydrogenation percentage that only requires a comparison between two 1-hexene TPD spectra, one of which is taken at an exposure larger than one monolayer. One only has to assume that the sticking coefficient in the monolayer and multilayer are the same at the substrate dosing temperature. This is a reasonable assumption in nearly all cases involving gaseous organic molecules at room temperature colliding with a metal substrate at 100 K.[36] After an exposure A that gives a physisorbed molecular desorption peak area S_{phys_A} and chemisorbed molecular desorption peak area S_{chem_A}, one can calculate the peak area S_{total_A} by using $S_{total\_A} = S_{phys\_A} + S_{chem\_A}$. A measurement of the amount of adsorbed molecules that decompose θ_{dec_A} is also required, and this was obtained from the H_2 TPD spectra in this case. Similar parameters are then obtained after a different exposure B. The following equation can then be used to obtain the value for a variable denoted as X, which is the derived factor that converts the molecular TPD area into units of coverage:

$$\frac{A}{B} = \frac{\left(\frac{S_{total\_A}}{X} + \theta_{dec\_A}\right)}{\left(\frac{S_{total\_B}}{X} + \theta_{dec\_B}\right)} \quad (1)$$

The monolayer saturation coverage (θ_{sat}) on the surface can then be calculated from $(S_{chem\_A})/(X) + \theta_{dec\_A}$ and the percentage dehydrogenation is given by $(\theta_{dec\_A})/(\theta_{sat}) \times 100\%$. Using this method, we calculated a monolayer saturation coverage of 1-hexene on Pt(111) of 0.19 ML, which is identical with that obtained from Figure 6.

3.3. 1,5-Hexadiene, C_6H_{10}. TPD spectra for 1,5-hexadiene desorption were obtained by monitoring the signal at 67 amu, the major cracking fraction peak from 1,5-hexadiene in the QMS, after 1,5-hexadiene exposures on Pt(111) at 110 K. Some of these are given in Figure 7a. After small exposures, no molecular 1,5-hexadiene desorption was observed, and only H_2 was liberated from surface. Signals at 86, 84, 82, 78, 28, and 2 amu were monitored to search for other desorbed products. Larger exposures of 1,5-hexadiene lead to a peak at 227 K. One would expect that 1,5-hexadiene has a much stronger interaction (nearly twice as strong) with Pt(111) than 1-hexene because it contains an additional C═C double bond. The desorption peak at 227 K corresponds to a desorption activation energy of only 58 kJ/mol, which is 15 kJ/mol lower than that for 1-hexene chemisorbed on Pt(111) and almost the same value as that for 1-hexane adsorbed on Pt(111). This indicates that this peak is not from the chemisorbed monolayer. Increasing the exposure eventually caused formation of a second layer from which species desorb at 157 K. A multilayer desorption peak at 132 K was also observed at higher exposures (not shown). Since the desorption peak at 227 K is not assigned to the chemisorbed

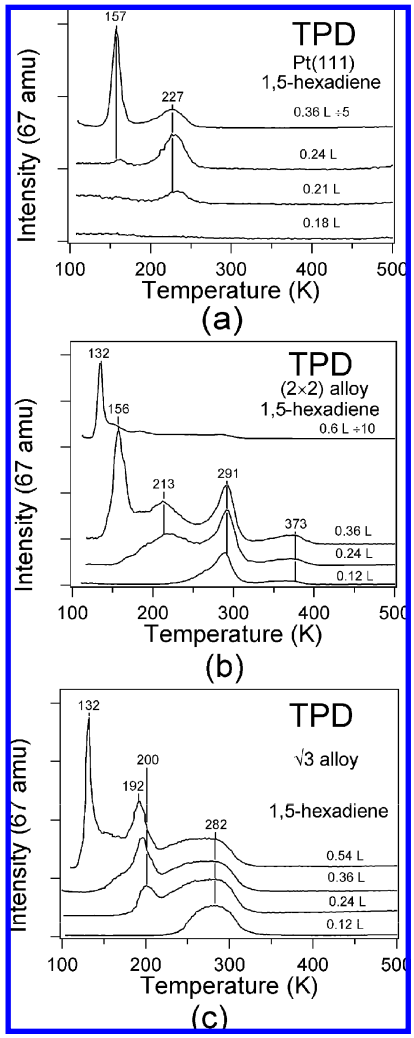

Figure 7. 1,5-Hexadiene (C_6H_{10}) TPD traces following 1,5-hexadiene exposures on (a) Pt(111) and the (b) (2 × 2)-Sn/Pt(111) and (c) ($\sqrt{3}$ × $\sqrt{3}$)R30°-Sn/Pt(111) alloys at 110 K.

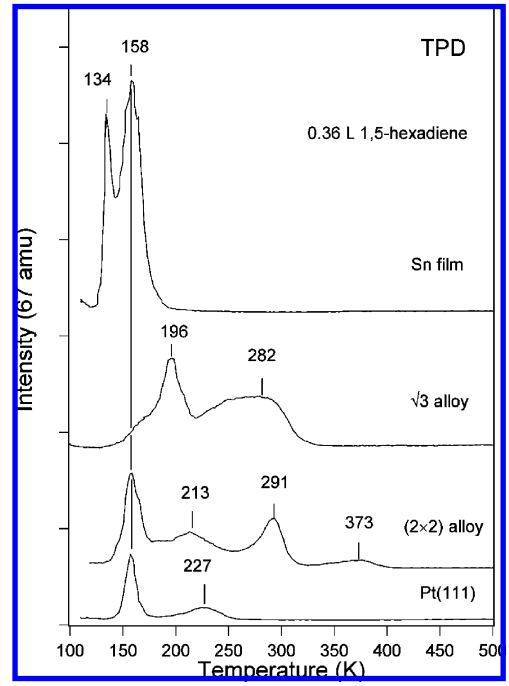

Figure 8. Comparison of the 1,5-hexadiene (C_6H_{10}) TPD curves after 0.36 L 1,5-hexadiene exposures that produce coverages near one monolayer on Pt(111), the (2 × 2)-Sn/Pt(111) and ($\sqrt{3}$ × $\sqrt{3}$)R30°-Sn/Pt(111) alloys, and a thick Sn film at 110 K.

monolayer and no desorption peak higher than 227 K was observed, we conclude that chemisorbed 1,5-hexadiene fully dehydrogenated during TPD.

1,5-Hexadiene TPD spectra after increasing 1,5-hexadiene exposures on the (2 × 2) alloy are given in Figure 7b. Molecular 1,5-hexadiene desorption from the chemisorbed monolayer was observed even at low exposures in two peaks at 373 (E_d = 96 kJ/mol) and 291 K (E_d = 75 kJ/mol). Increasing the exposure led to a new peak at 213 K, which is close to the peak at 227 K seen for 1,5-hexadiene on Pt(111). Large exposures caused the formation of a second layer, which desorbed at 156 K and a multilayer desorption peak at 132 K.

A series of 1,5-hexadiene TPD spectra that were obtained after 1,5-hexadiene exposures on the $\sqrt{3}$ alloy is shown in Figure 7c. Desorption from the chemisorbed monolayer was initially observed in a broad peak at 282 K (E_d = 72 kJ/mol) after small exposures, but larger exposures led to a new peak at 192−200 K. Species present in the multilayer desorb at 132 K.

Figure 8 compares 1,5-hexadiene desorption on Pt(111), the (2 × 2) and $\sqrt{3}$ alloys, and a thick Sn film. Alloying Sn with Pt(111) inhibited dehydrogenation of chemisorbed 1,5-hexadiene, and this led to increased high temperature molecular desorption. Desorption in four peaks, in addition to the multilayer peak at 134 K, was observed in TPD from the (2 × 2) alloy. These peaks appear at 373, 291, 213, and 158 K with E_d = 96, 75, 54, and 39 kJ/mol, respectively. These multiple peaks mean that 1,5-hexadiene had several different chemisorption states on the (2 × 2) alloy. On the $\sqrt{3}$ alloy, the broad 1,5-hexadiene desorption peak around 282 K corresponds to a desorption activation energy of 72 kJ/mol, which is 17 kJ/mol larger than that of 1-hexene on the $\sqrt{3}$ alloy. The desorption peak at 196 K (E_d = 50 kJ/mol) on the $\sqrt{3}$ alloy is close to that of 1-hexene on the same surface. 1,5-Hexadiene only has a weak adsorption interaction on a thick Sn film and desorbs at the same temperature as *n*-hexane and 1-hexene.

A saturation coverage of 0.13 ML for 1,5-hexadiene adsorption on Pt(111) can be calculated from the H_2 TPD spectra assuming complete dehydrogenation of the chemisorbed monolayer. By using the second method introduced above, we calculated that the monolayer saturation coverages of 1,5-hexadiene on the (2 × 2) and $\sqrt{3}$ alloys were 0.14 and 0.20 ML, respectively.

H_2 TPD spectra from the dehydrogenation of chemisorbed 1,5-hexadiene on Pt(111) are shown in Figure 9a. H_2 evolution was saturated after a 1,5-hexadiene exposure of 0.24 L. The H_2 desorption profile had five main peaks: 285, 383, 413, 488, and 585 K at large coverages. The lowest temperature H_2 desorption from the dehydrogenation of 1,5-hexadiene is likely to be H_2-desorption rate-limited, because H_2 desorption from H_2 exposures occurs at about 350 K. This conclusion is sensible because 1,5-hexadiene should be at least as reactive as 1-hexene. H_2 desorption peaks above 350 K represent reaction-rate limited production of H_2. The H_2 desorption peaks had an area ratio of 3.5:3.5:3 for desorption at temperatures below 350 K, 350−450 K, and above 450 K, indicating that 1,5-hexadiene lost either 3 or 4 H atoms during the first step (or steps) of dehydrogenation.

Figure 9b provides a summary of H_2 desorption from 1,5-hexadiene dehydrogenation. No H_2 desorption was observed from the $\sqrt{3}$ surface alloy, while 32% of the amount of H_2 evolved from Pt(111) was desorbed from the (2 × 2) alloy.

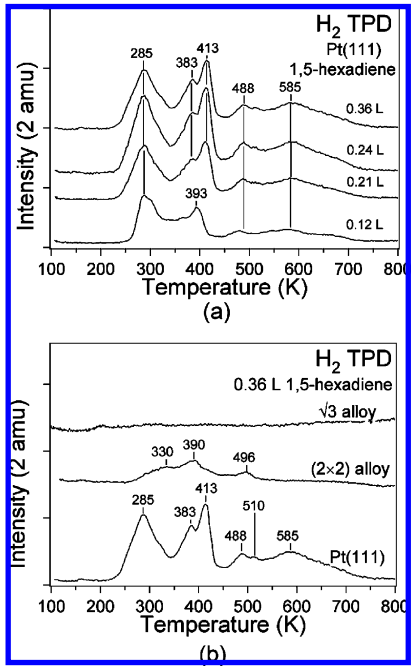

Figure 9. (a) H_2 TPD traces resulting from 1,5-hexadiene dehydrogenation after 1,5-hexadiene exposures on Pt(111) at 110 K. (b) Comparison of the H_2 TPD curves after 0.36 L 1,5-hexadiene exposures that produce coverages near one monolayer on Pt(111) and the (2 × 2)-Sn/Pt(111) and ($\sqrt{3}$ × $\sqrt{3}$)R30°-Sn/Pt(111) alloys at 110 K.

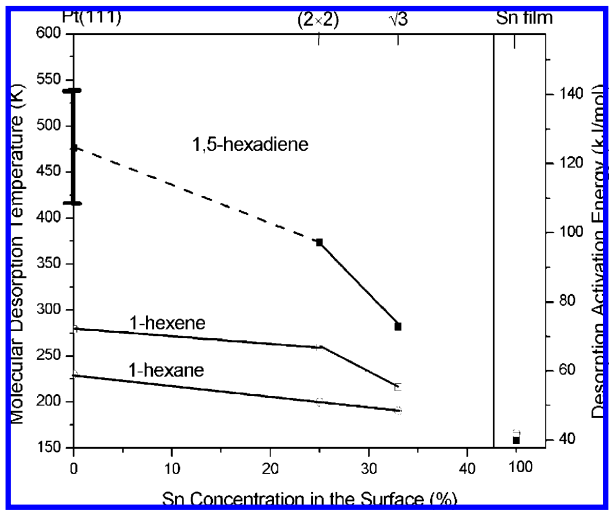

Figure 10. Plot of the peak temperatures observed in TPD for molecular desorption after *n*-hexane, 1-hexene, and 1,5-hexadiene exposures to produce submonolayer coverages on Pt(111), the (2 × 2)-Sn/Pt(111) and ($\sqrt{3}$ × $\sqrt{3}$)R30°-Sn/Pt(111) alloys, and a thick Sn film at 110 K. The right-hand axis gives an estimate of the corresponding molecular desorption activation energies as derived from a simple Redhead analysis.

Dehydrogenation of 1,5-hexadiene on the (2 × 2) alloy resulted primarily in three broad, H_2-desorption peaks at 330, 390, and 496 K, and this H_2 yield corresponds to dehydrogenation of 30% of the monolayer saturation coverage of 1,5-hexadiene. The amount of residual carbon detected by AES measurements after these TPD experiments on both the (2 × 2) and the $\sqrt{3}$ alloys was consistent with these results.

Figure 10 and Figure 11 summarize the quantitative aspects of our results for *n*-hexane, 1-hexene, and 1,5-hexadiene adsorption, desorption, and reaction on Pt(111), the (2 × 2) and $\sqrt{3}$ alloys, and a Sn film, specifically evaluating the influence of the amount of alloyed Sn on these results. Figure

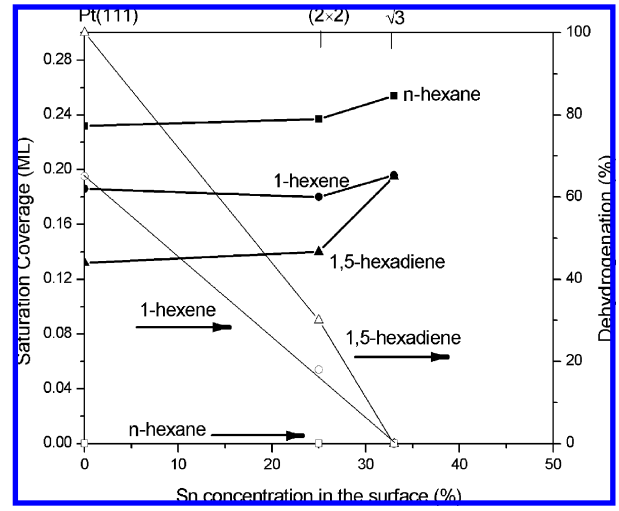

Figure 11. Plots of the monolayer saturation coverage (left-hand axis; solid points) and dehydrogenation percentage (right-hand axis; open points) following adsorption of *n*-hexane, 1-hexene, 1,5-hexadiene monolayers on Pt(111), and the (2 × 2)-Sn/Pt(111) and ($\sqrt{3}$ × $\sqrt{3}$)R30°-Sn/Pt(111) alloys at 110 K.

10 provides plots of the molecular desorption peak temperatures and corresponding activation energies for *n*-hexane, 1-hexene, 1,5-hexadiene desorption. Peak temperatures at submonolayer coverages were used to construct this plot. The temperature and activation energy of the higher of the two desorption peaks observed for 1-hexene and 1,5-hexadiene on the two alloys is plotted in Figure 10. Our results for the adsorption and desorption of all three molecules on a thick Sn film confirms that all of these molecules have only a very weak interaction with metallic Sn atoms and Sn was inactive for activating any bonds in these molecules. Furthermore, *n*-hexane, 1-hexene, and 1,5-hexadiene have similar E_d values on a thick Sn film. Figure 11 gives plots of the saturation coverage (left-hand axis; solid points) and dehydrogenation percentage (right-hand axis; open points) for all three molecules versus the surface Sn concentration. A detailed discussion of these figures is provided in Discussion below.

4. Discussion

4.1. Adsorption and Desorption of *n*-Hexane. Adsorption of *n*-hexane on Pt(111) and two Sn/Pt(111) surface alloys was completely reversible. Previous work by Chesters and coworkers[22] using RAIRS was interpreted in terms of a preference by *n*-hexane for an adsorption geometry in which it is lying "flat" on Pt(111) with the hydrocarbon backbone parallel to the surface plane. The presence of Sn in the surface layer of these Sn/Pt(111) alloys decreased the interaction of *n*-hexane with the surface, that is, lowered the adsorption energy, which was measured in these experiments by the decreased activation energy for *n*-hexane desorption. This is illustrated in Figure 10. Similar effects have been seen previously for butane,[23] cyclohexane,[24] and other alkanes adsorbed on these Sn/Pt(111) alloys. A small, linear decrease in the desorption activation energy occurs for all of the alkanes and cycloalkanes investigated, with a very similar slope for increasing Sn concentration. It is worth noting that *n*-hexane desorbed from these two Sn/Pt(111) alloys in a single, narrow peak. This observation suggests that the Sn/Pt(111) surface alloys can be prepared to be quite homogeneous in composition and structure, with few defects beyond those inherent to typical surfaces of metal single-crystal samples.

In contrast to its effect on adsorption energies, the presence of alloyed Sn did not reduce the monolayer saturation coverage

of *n*-hexane from that on Pt(111) and apparently even increased it slightly (10%) on the $\sqrt{3}$ alloy. This is shown in Figure 11. Sn has been referred to commonly as an inert site-blocking component in discussing the hydrocarbon conversion chemistry that occurs on Pt−Sn bimetallic catalysts.[15,18] Our results show that Sn on these two alloys has no site-blocking effect on the initial elementary step in the catalysis of alkane conversion, that is, adsorption of the alkane reactant as probed here by *n*-hexane adsorption at low temperatures.

On Pt(111), *n*-hexane and cyclohexane have the same desorption activation energies, indicating similar adsorption interactions with the surface. However, cyclohexane is more reactive than *n*-hexane on Pt(111), and cyclohexane starts to dehydrogenate at 180−195 K and forms benzene at 270−340 K in the dehydrogenation process. *n*-Hexane does not undergo any dehydrogenation during heating in TPD following *n*-hexane adsorption on Pt(111). These observations illustrate that the C−H bond-breaking barrier of alkanes and cycloalkanes is different on Pt(111).

4.2. 1-Hexene Adsorption and Reaction. The desorption of chemisorbed 1-hexene on Pt(111) occurs in a peak at 279 K, which is very close to the ethylene desorption peak in TPD at 284 K.[25] This result indicates that 1-hexene is similarly di-σ-bonded to Pt(111) at low temperatures and the Pt−C bond strength only slightly decreases upon substitution of alkyl groups for H atoms in the ethylene molecule. Similar results were also observed previously for propene[26] and 1-butene.[27] The 1-hexene TPD spectra in Figure 3a reveal another desorption peak at 162 K near monolayer saturation coverage, and this peak did not increase substantially with larger exposures. This observation implies that we should not simply assign this peak to desorption of physisorbed molecules adsorbed in the second layer. Similar low-temperature peaks were also observed after 1-butene and isobutene[27] adsorption on Pt(111), but no such features were observed for ethylene and propene.[26] It is possible that this peak arises from molecules that chemisorb on the Pt(111) surface but that are only weakly π-bonded because of hindered access to preferred adsorption sites on the surface because of the presence of di-σ-bonded coadsorbed species at high coverages.

The first step in 1-hexene dehydrogenation is formation of surface-bound hexylidyne ($Pt_3{\equiv}C{-}(CH_2)_4{-}CH_3$), as observed at 250 K by using RAIRS.[22] Hexylidyne species partially dehydrogenate at 270 K to form a metallacycle ($Pt_3{\equiv}C{-}(CH_2)_5{-}Pt$) intermediate. The H atom generated in this step is coadsorbed with the metallacycle on Pt(111) and is released upon further heating, which corresponds to the two desorption rate-limited peaks at 293 and 313 K in H_2 TPD traces. Forming surface-bound alkylidyne ($Pt{\equiv}C{-}R$) groups as stable intermediates in 1-alkene dehydrogenation on Pt(111) is a general pathway that has been observed also for ethylene,[25] propene,[26] and 1-butene.[27]

As previously observed for other alkenes, the desorption activation energy of 1-hexene was reduced, as shown in Figure 10, and dehydrogenation of 1-hexene was greatly suppressed, as shown in Figure 11, by the presence of alloyed Sn at the Pt(111) surface. H_2 desorption in TPD studies is a convenient and accurate monitor of 1-hexene dehydrogenation since no other products were observed in TPD (e.g., alkanes) on any of the three substrates. The attenuation of the amount of dehydrogenation is much larger than the reduction of the 1-hexene adsorption energy and is proportional to the surface Sn concentration over this range of Sn coverages. Replacing 25% of the surface Pt atoms with alloyed Sn atoms reduces by 73% the H_2 evolution compared with that from Pt(111). No H_2 evolution was observed during TPD from the $\sqrt{3}$ alloy, and thus, no dehydrogenation of 1-hexene occurred. In principle, this may be caused by the decreased adsorption energy of 1-hexene on the alloys, which would enhance the branching ratio of molecular desorption over dehydrogenation without a change in the energetic barrier to dehydrogenation, but our work with large (strongly adsorbed) alkenes shows that the decrease in the amount of dehydrogenation is due to an increased C−H bond scission barrier on the alloys over that on Pt(111). The origin of this increase could be due to the absence of adjacent pure-Pt 3-fold sites or the decreased number of pure-Pt 3-fold sites caused by alloying Sn (ensemble effects), or due to electronic effects. In addition to altering the availability of pure-Pt sites, alloying also changes the local electronic structure at Pt sites. Calculations by Pick[37] and Delbecq and Sautet[38] found that a shift of the Pt *d*-band center resulted from charge transfer from Sn to Pt and this decreased the bond strength between adsorbed molecules and Sn−Pt alloys. Such changes should also lead to an even larger increase in activation energy barriers for bond dissociation reactions of adsorbed molecules.

It is always very difficult to separate geometric (ensemble) and electronic (ligand) effects and perhaps futile when reactive ensembles are just a few (<5) Pt atoms, yet it remains attractive to cling to the possibility that chemical reactivity can be accounted for and predicted by simply looking at the nature of the reactive sites (ensembles) on alloys (because this might avoid the need for new, highly accurate calculations for every alloy combination and structure). No adjacent pure-Pt 3-fold hollow sites are present on the (2 × 2) alloy, and no pure-Pt 3-fold hollow sites exist at all on the $\sqrt{3}$ alloy. Strong bonding of alkylidyne intermediates formed from alkene dehydrogenation would seem to require at least the presence of pure-Pt 3-fold sites, and this may explain why small alkene molecules have much lower dehydrogenation activity on the $\sqrt{3}$ alloy. Alloying Sn on Pt(111) to form these ordered surface alloys reduces the number of pure-Pt 3-fold sites from $\theta_{Pt3} = 2$ ML on Pt(111) (note there are two hollow sites within each primitive unit cell on the clean surface) to $\theta_{Pt3} = 0.5$ ML on the (2 × 2) alloy and $\theta_{Pt3} = 0$ ML on the $\sqrt{3}$ alloy. Thus, inherently, there is a linear proportionality between θ_{Pt3} and θ_{Sn} for these two ordered alloys. Our results, shown in Figure 11, demonstrated that the dehydrogenation percentage of 1-hexene was linearly proportional to θ_{Sn}. A possible origin of this effect is the number of pure-Pt 3-fold sites, as shown in Figure 12. This correlation suggests that a reactive ensemble effect can account for the reactivity of 1-hexene, and other alkene molecules with β-hydrogens, on such Pt−Sn alloys without a detailed knowledge of the subtle electronic effects. That is not to say that there are no electronic effects, indeed a plot of the dehydrogenation percentage of 1-hexene versus the *d*-band center (Pt = −1.93, Pt_3Sn = −2.09, and Pt_2Sn = −2.12 eV[37,38]) is also linear. Further work is required to explain fully this "site-directed" chemistry.

Unlike other alkene molecules studied before, two desorption peaks were observed in TPD experiments after 1-hexene adsorption to form a chemisorbed monolayer on the (2 × 2) and $\sqrt{3}$ alloys. These desorption peaks correspond to desorption activation energies of 66 and 62 kJ/mol on the (2 × 2) alloy, and these values are reduced to 55 and 50 kJ/mol on the $\sqrt{3}$ alloy. We consider that the difference of 5−6 kJ/mol in the desorption energy (equal to the adsorption energy for nonactivated adsorption, as is the case here) is too small to be accounted for by the difference between di-σ-bonded and π-bonded species. Thus, we do not assign the lower temperature desorption peak from the monolayer to simply the presence of π-bonded

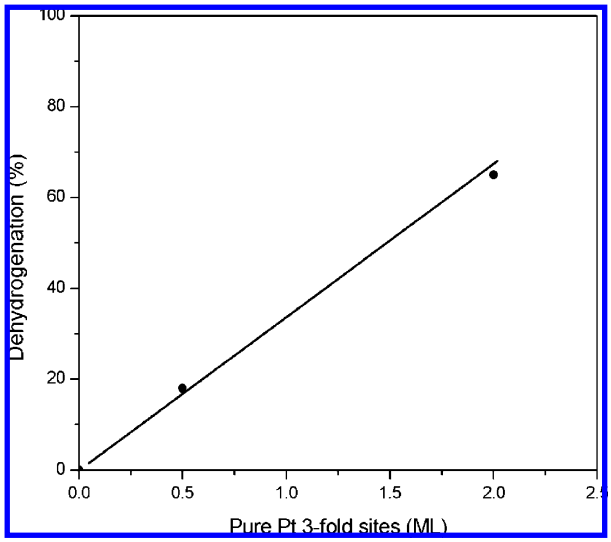

Figure 12. Dehydrogenation percentage of 1-hexene increases linearly with the number of pure-Pt 3-fold sites.

1-hexene chemisorbed in the monolayer on both alloys. Since pure-Pt 3-fold, pure-Pt 2-fold, and Pt atop sites have different interactions with adsorbed molecules, we assign this peak to 1-hexene desorption from less-active sites, such as pure-Pt 2-fold, and Pt atop sites that are not typically populated on the clean Pt(111) surface. Particularly, repulsive interactions of the longer alkyl side chain of 1-hexene over that of 1-butene, propene, and especially ethylene may force some 1-hexene to form a di-σ-bonded species located on a less-active, or less strongly binding, site.

To the extent that the Pt−Sn alloy phases in our study resemble those catalytically active sites on a working catalyst, such as that reported on by Llorca et al.,[17] our results provide an explanation for the improvement in the catalytic selectivity to 1-hexene in *n*-hexane dehydrogenation with increasing Sn concentration. Decreased 1-hexene dehydrogenation activity on Pt−Sn alloys increases the selectivity for gas-phase 1-hexene production and also increases the catalyst lifetime by reducing carbon buildup due to nonspecific dehydrogenation that gradually poisons the catalyst surface. Weaker 1-hexene chemisorption provides a shorter lifetime of 1-hexene on the catalyst surface and reduces the chance of further nonselective competing reactions.

4.3. Adsorption and Reaction of 1,5-Hexadiene. Like butadiene,[39] chemisorbed 1,5-hexadiene dehydrogenates completely on Pt(111) during heating in TPD experiments. The thermal desorption peak of 1,5-hexadiene from Pt(111) at 227 K is at a temperature that is much lower than that of chemisorbed 1-hexene and is close to that of chemisorbed 1-hexane. So, it is reasonable that this peak should not be assigned to desorption of chemisorbed 1,5-hexadiene, but its origin is not clear. A similar peak was not observed in TPD studies of butadiene, which is a molecule that should have a more "flat" adsorption geometry than 1,5-hexadiene. We propose that the peak at 227 K arises because of 1,5-hexadiene desorption from second-layer molecules, but those where a significant polarization interaction exists with the Pt(111) surface that exceeds that of most second-layer physisorbed species are completely shielded from the metal surface by molecules in the chemisorbed monolayer.

Alloying Sn into the Pt(111) surface greatly suppressed the dehydrogenation of 1,5-hexadiene compared with that on the clean Pt(111) surface. The H_2 yield from the (2 × 2) alloy during heating of the 1,5-hexadiene monolayer is only 30% of that produced from Pt(111), and dehydrogenation is completely blocked on the $\sqrt{3}$ alloy. This is consistent with a proposal that dehydrogenation of 1,5-hexadiene requires pure-Pt 3-fold hollow sites. However, electronic effects may also be responsible for the increased C−H bond-breaking barrier on the alloys and the relative importance of the two effects cannot be deduced at this time.

The 1,5-hexadiene desorption peak at 373 K from the (2 × 2) alloy is broad, which indicates that the molecule has variable interaction energies with the surface; that is, one or both of the C=C double bonds interacts to varying degrees with the surface because of a variety of adsorption geometries or configurations. The value of E_d corresponding to the peak at 373 K on the (2 × 2) alloy is 96 kJ/mol, which is 8 kJ/mol larger than that of 1,3-butadiene on the same alloy.[39] This E_d value is 1.5 times that for 1-hexene on the (2 × 2) alloy, and this is the same E_d ratio that was observed between 1,3-butadiene and 1-butene on the (2 × 2) alloy. We propose that 1,5-hexadiene desorption in a peak at 373 K is from a chemisorbed state of 1,5-hexadiene in which both C=C double bonds in the molecule are now di-σ-bonded to the surface but in a fashion where the carbon atoms are less sp^3-rehybridized than that on Pt(111). The 1,5-hexadiene desorption peak at 291 K is much larger and narrower than the one at 373 K. This lower temperature peak has E_d = 75 kJ/mol, and this is only 9 kJ/mol larger than the E_d value for 1-hexene chemisorbed on the (2 × 2) alloy. This indicates that 1,5-hexadiene desorption in the peak at 291 K is from a chemisorbed state of 1,5-hexadiene in which only one C=C double bond in the molecule is di-σ-bonded to the surface and that the second C=C double bond in 1,5-hexadiene has only a weak interaction with the surface.

The 1,5-hexadiene desorption peak at 282 K from the $\sqrt{3}$ alloy is very broad. The desorption activation energy of this peak of 72 kJ/mol is only 17 kJ/mol larger than that of 1-hexene on the same surface. This suggests that the second C=C double bond in 1,5-hexadiene has only a weak interaction with the $\sqrt{3}$ alloy surface. This is different behavior than was observed for chemisorbed butadiene, which had a much narrower desorption peak in TPD from the $\sqrt{3}$ alloy. E_d for butadiene is 1.5 times that of 1-butene on the $\sqrt{3}$ alloy. The weak interaction between the second C=C double bond in 1,5-hexadiene and the alloy surface may be caused by structural limitations. Formation of one di-σ-bond to the alloy surface apparently limits the interaction of the second C=C double bond. On the $\sqrt{3}$ alloy, the 1,5-hexadiene desorption peak at 196 K has the same E_d value as that for the 1-hexene TPD peak obtained at saturation coverage. This indicates that 1,5-hexadiene desorbing in this peak was only interacting with the $\sqrt{3}$ alloy via one C=C double bond, and the second C=C double bond had no appreciable interaction with the surface.

During heating in TPD of a 1,3-cyclohexadiene monolayer on both the (2 × 2) and the $\sqrt{3}$ alloy, 1,3-cyclohexadiene completely dehydrogenates to evolve gas phase benzene and H_2.[28] Herein, we have shown that 1,5-hexadiene only partially dehydrogenated to liberate H_2 on the (2 × 2) alloy, and it reversibly chemisorbed on the $\sqrt{3}$ alloy. No gas-phase benzene was produced; that is, no cyclization of 1,5-hexadiene was detected on either of these two alloys. These observations indicate that the activation barrier to forming new C−C bonds is higher than the 1,5-hexadiene desorption barrier on both alloys and is also higher than the C−H bond-breaking barrier on the (2 × 2) alloy. Dehydrogenation of 1,3-cyclohexadiene evidently allows facile transformation to a benzene product, without

having to surmount the higher energy C−C bond-forming barrier required for producing benzene from 1,5-hexadiene. Dehydrogenation of 1,5-hexadiene leads to unreactive "dead end" alkylidyne species that subsequently cannot be dehydrogenated further to produce benzene.

4.4. Influence of the Degree of Unsaturation in Linear C_6 Molecules on Adsorption and Reaction on Sn/Pt(111) Alloys. Figure 10 summarizes the molecular desorption temperatures and corresponding desorption activation energies E_d of *n*-hexane, 1-hexene, and 1,5-hexadiene. An E_d value for 1,5-hexadiene on Pt(111) was estimated to be between an upper limit suggested by using two times the E_d value of 1-hexene, which assumes that 1,5-hexadiene is tetra-σ-bonded to Pt(111), and a lower limit obtained by using the measured result of 1.5 times the E_d value of 1-hexene on the (2 × 2) alloy, which assumes that each π-bond in the gas-phase 1,5-hexadiene molecule only interacts with Pt(111) as strongly as on the (2 × 2) alloy. Just as was observed for 1-butane,[23] the *n*-hexane desorption peak temperature decreased linearly with increased Sn concentration to 0.33. UPS spectra of these alloys[40] show only small changes in the Pt valence band and a change in the work function compared with that on Pt(111). Alkanes form only weak dispersion or H-bonding interactions with the surface, probing the polarizability of the surface and showing only a weak dependence on the surface Sn concentration that appears to be proportional to the amount of Sn in this range. This is not the behavior observed, however, for 1-hexene, and a relatively larger effect on its adsorption energy was observed upon forming the $\sqrt{3}$ alloy. Such a change is consistent with that seen for all of the alkenes studied previously.[25−27] The effect of alloying Sn into the Pt(111) surface to form the (2 × 2) alloy only decreases the adsorption energy of 1-hexene about the same amount as that for *n*-hexane. This means that the sites necessary for strong alkene chemisorption are not strongly affected by this alloying. However, in changing from the (2 × 2) to $\sqrt{3}$ alloy structure, a larger effect on the 1-hexene adsorption energy occurred than would have been expected from the effects of simply adding additional Sn atoms in the alloy. We can associate this change as arising from the loss of pure-Pt 3-fold hollow sites on the $\sqrt{3}$ alloy and their importance in strongly chemisorbing alkenes.

On the $\sqrt{3}$ alloy, the small difference between the E_d values of 1,5-hexadiene and those of 1-hexene in Figure 10 indicates that 1,5-hexadiene did not form a tetra-σ-bonded adsorption complex as it does on Pt(111). Whether or not this bonding geometry exists on the (2 × 2) alloy is not clear, because this species may not desorb molecularly in TPD but rather dehydrogenate. The decrease in E_d observed for 1,5-hexadiene upon changing from the (2 × 2) to $\sqrt{3}$ alloy was larger than that for 1-hexene.

Alloying Sn into the Pt(111) surface decreased the adsorption energies of all three molecules. Addition of $\theta_{Sn} = 0.25$ ML and formation of the (2 × 2) alloy affected all three molecules similarly, independent of the degree of unsaturation, specifically the number of C=C bonds, in the molecule. However, the effect of forming the $\sqrt{3}$ alloy by the addition of $\theta_{Sn} = 0.33$ ML depended on the degree of unsaturation in the molecule. Increased numbers of C=C double bonds in linear C_6 hydrocarbons caused an increasing influence on adsorption energies when changing the surface from a (2 × 2) to a $\sqrt{3}$ alloy.

Figure 11 summarizes the saturation coverage and amount of dehydrogenation for *n*-hexane, 1-hexene, and 1,5-hexadiene on the surfaces investigated. The monolayer saturation coverage decreases with an increased number of C=C double bonds in these three linear C_6 hydrocarbons on both Pt(111) and the (2 × 2) alloy. However, on the $\sqrt{3}$ alloy, the monolayer coverage of 1-hexene and 1,5-hexadiene are the same and smaller than that of 1-hexane. Also, we note that, for any given molecule, alloying Sn to the surface over this range does not decrease the monolayer saturation coverage of that molecule, as might have been expected from a simplistic site-blocking argument, and is even increased (especially for 1,5-hexadiene) on the $\sqrt{3}$ alloy. Such observations were also made in previous studies of other alkane and alkene molecules.[23,26,27] We explain the decrease in the monolayer coverage with an increased number of C=C double bonds in these molecules on Pt(111) and the (2 × 2) alloy as arising from the constraints on the strong specific bonding interactions that must occur at specific sites to enable strong chemisorption bonding and the increased difficulty of satisfying these constraints at high coverages. That is, more C=C double bonds in the molecule will lead to a lower density in the adsorbed monolayer because even though "Pt area" is still available at high coverages, that is, the molecules are not close-packed in two dimensions, this Pt area does not contain enough space to accommodate another molecule coordinated with the C=C double bond located at the specific site required for strong chemisorption. The increase in the monolayer coverage of all of these molecules, especially 1,5-hexadiene, on the $\sqrt{3}$ alloy is explained as arising from a small relaxation of the bonding geometry/site requirements that result from weaker bonding interactions between the molecules and the $\sqrt{3}$ alloy surface.

Figure 11 also shows the amount of dehydrogenation of these hydrocarbons that occurs during TPD obtained at monolayer coverages on the surfaces investigated. *n*-Hexane is reversibly adsorbed on all three surfaces under UHV conditions, and no decomposition was detected during TPD. The greater reactivity of 1-hexene over that of *n*-hexane and the increased percentage of dehydrogenation of 1,5-hexadiene over that of 1-hexene on Pt(111) and the (2 × 2) alloy illustrates the increased reactivity on these surfaces that occurs with an increasing number of C=C double bonds in hydrocarbon adsorbates. The decomposition of all three of these linear C_6 hydrocarbons was eliminated on the $\sqrt{3}$-alloy surface. We explained (in section 4.2. using Figure 12) that this change could be accounted for by the loss of pure-Pt 3-fold hollow sites on the $\sqrt{3}$ alloy and their importance in activating the C−H bond breaking required for dehydrogenation. In the particular case of 1-hexene, there is a linear relationship between the amount of dehydrogenation and the number of pure-Pt 3-fold hollow sites available at the surface. 1,5-hexadiene is slightly more reactive on the (2 × 2) alloy than would be expected on this basis alone.

5. Conclusions

Chemisorption and reactivity studies were carried out to probe how the degree of unsaturation affects the adsorption energy and reactivity of linear C_6 hydrocarbons on Pt and Pt−Sn alloys. On Pt(111), increasing the number of C=C double bonds in the molecule led to a large increase in the adsorption energy and reactivity of linear C_6 hydrocarbons. *n*-Hexane adsorbed reversibly on Pt(111), but 1,5-hexadiene completely decomposed on Pt(111) to liberate H_2 and produce surface carbon upon heating in TPD measurements. For 1-hexene, which is chemisorbed in a di-σ-bonding geometry on Pt(111) at low temperature, 65% of the adsorbed monolayer decomposed upon heating in TPD. Our investigations then revealed how these strong effects were altered by the presence of alloyed Sn at the Pt(111) surface. In particular, two ordered alloys were utilized, Pt(111) and two ordered surface alloys, a (2 × 2)-Sn/Pt(111) surface

with $\theta_{Sn} = 0.25$ and a $(\sqrt{3} \times \sqrt{3})$R30°-Sn/Pt(111) surface with $\theta_{Sn} = 0.33$, so that the reactive sites present at the bimetallic surface could be clearly identified. Alloying Sn with Pt(111) had only a minimal influence on the behavior of *n*-hexane. The adsorption energy of *n*-hexane decreased weakly and linearly with increasing Sn concentration in the surfaces of these alloys. This behavior arises from the weak dispersion or H-bonding interactions between the *n*-hexane and the metal surface. The single, well-defined *n*-hexane desorption peak at characteristic temperatures on each surface indicates that the alloys can be prepared with a largely uniform composition and structure.

Increasing the degree of unsaturation in the molecule alters this situation, and in contrast to *n*-hexane, alloying with Sn has a significant influence on the adsorption and reactivity of 1-hexene and 1,5-hexadiene. Increasing the surface Sn concentration most strongly decreased the adsorption energy of 1,5-hexadiene, but this influence was nonlinear in the amount of Sn for both 1-hexene and 1,5-hexadiene. The most significant alteration caused by alloying Sn was on the dehydrogenation activity of the alloys for both 1-hexene and 1,5-hexadiene. The amount of dehydrogenation that occurred during heating in TPD measurements of 1-hexene and 1,5-hexadiene monolayers was reduced from 65 and 100% on Pt(111) to 18 and 30% on the (2 × 2)-Sn/Pt(111) alloy, respectively. Dehydrogenation activity for both molecules was totally eliminated on the $(\sqrt{3} \times \sqrt{3})$R30°-Sn/Pt(111) alloy. Reversible alkene and diene adsorption was associated with the elimination of pure-Pt 3-fold sites on the $(\sqrt{3} \times \sqrt{3})$R30°-Sn/Pt(111) alloy. Furthermore, the decrease in the amount of 1-hexene dehydrogenation on these three surfaces was linearly related to the decrease in the number of pure-Pt 3-fold sites. In this case, this correlation illustrates the importance of a geometric or ensemble effect in accounting for the reactivity of these surfaces. Such structure−reactivity correlations are an important component in advancing a description of the "site-directed" chemistry of such bimetallic surfaces.

Increasing the number of C═C double bonds in these linear C_6 hydrocarbons served, in general, to decrease the monolayer saturation coverage of these molecules on Pt(111) and the two alloy surfaces. We proposed that this was due to the increased site requirements for strong chemisorption bonding that are introduced with each C═C double bond in the molecule and the role that this plays in forming less tightly packed monolayers on a given surface. Alloying Sn with Pt(111) had only a minimal influence on the monolayer saturation coverage of these molecules, and if any, increased the coverages slightly because of reducing the bonding interactions with the surface and relaxing slightly the site constraints.

Acknowledgment. This material is based upon work supported by the National Science Foundation under Grant 0616644. The authors thank Lindsey A. Welch for a careful review of the manuscript and helpful comments.

References and Notes

(1) Paál, Z. *Adv. Catal.* **1980**, *29*, 273.
(2) Gault, F. G. *Adv. Catal.* **1981**, *30*, 1.
(3) Maire, G.; Garin, F. In *Catalysis Science and Technology*; Anderson, J. R., Boudart, M., Eds.; Springer: Berlin, 1984; Vol. 6, p 161.
(4) Paál, Z.; Brose, B.; Räth, M.; Gombler, W. *J. Mol. Catal.* **1992**, *75*, L13.
(5) Dautzenberg, F. M.; Platteeuw, J. C. *J. Catal.* **1970**, *19*, 41.
(6) Paál, Z.; Tétényi, P. *Acta Chim. Acad. Sci. Hung.* **1967**, *54*, 175.
(7) Paál, Z.; Tétényi, P. *Acta Chim. Acad. Sci. Hung.* **1967**, *53*, 193.
(8) Paál, Z.; Tétényi, P. *J. Catal.* **1973**, *30*, 350.
(9) Paál, Z.; Xu, X. L. *Appl. Catal.* **1989**, *43*, L1.
(10) Völter, J.; Lietz, G.; Uhlemann, M.; Hermann, M. *J. Catal.* **1981**, *68*, 42.
(11) Burch, R.; Garla, L. C. *J. Catal.* **1981**, *71*, 360.
(12) Balakrishnan, K.; Schwank, J. *J. Catal.* **1991**, *127*, 287.
(13) Lieske, H.; Völter, J. *J. Catal.* **1984**, *90*, 96.
(14) Li, Y. X.; Stencel, J. M.; Davis, B. H. *Appl. Catal.* **1990**, *64*, 71.
(15) Dautzenberg, F. M.; Helle, J. N.; Biloen, P.; Sachtler, W. M. H. *J. Catal.* **1980**, *63*, 119.
(16) Fujikawa, T.; Ribeiro, F. H.; Somorjai, G. A. *J. Catal.* **1998**, *178*, 58.
(17) Lloca, J.; Homs, N.; Fierro, J. G.; Sales, J.; Piscina, P. R. *J. Catal.* **1997**, *166*, 44.
(18) Biloen, P.; Helle, J. N.; Verbeek, H.; Dautzenberg, F. M.; Sachtler, W. M. H. *J. Catal.* **1980**, *63*, 112.
(19) Paffett, M. T.; Windham, R. G. *Surf. Sci.* **1989**, *208*, 34.
(20) Chesters, M. A.; Gardner, P.; MoCash, E. M. *Surf. Sci.* **1989**, *209*, 89.
(21) Bishop, A. R.; Girolami, G. S.; Nuzzo, R. G. *J. Phy. Chem. B* **2000**, *104*, 754.
(22) Ilharco, L. M.; Garcia, A. R.; Hargreaves, E. C.; Chesters, M. A. *Surf. Sci.* **2000**, *459*, 115.
(23) Xu, C.; Koel, B. E.; Paffett, M. T. *Langmuir* **1994**, *10*, 166.
(24) Xu, C.; Tsai, Y. L.; Koel, B. E. *J. Phy. Chem.* **1994**, *98*, 585.
(25) Paffett, M. T.; Gebhard, S. C.; Windham, R. G.; Koel, B. E. *Surf. Sci.* **1989**, *223*, 449.
(26) Tsai, Y. L.; Xu, C.; Koel, B. E. *Surf. Sci.* **1997**, *385*, 37.
(27) Tsai, Y. L.; Koel, B. E. *J. Phy. Chem. B* **1997**, *101*, 2985.
(28) Peck, J. W.; Koel, B. E. *J. Am. Chem. Soc.* **1996**, *118*, 2708.
(29) Zhao, H.; Kim, J.; Koel, B. E. *Surf. Sci.* **2003**, *538*, 147.
(30) Overbury, S. H.; Mullins, D. R.; Paffett, M. T.; Koel, B. E. *Surf. Sci.* **1991**, *254*, 45.
(31) Redhead, P. *Vacuum* **1962**, *12*, 203.
(32) Windham, R. G.; Bartram, M. E.; Koel, B. E. *J. Phys. Chem.* **1988**, *92*, 2862.
(33) Salmeron, M.; Somorjai, G. A. *J. Phys. Chem.* **1982**, *86*, 341.
(34) Koestner, R. J.; Frost, J. C.; Stair, P. C.; Van Hove, M. A.; Somorjai, G. A. *Surf. Sci.* **1982**, *116*, 85.
(35) Avery, N. R.; Sheppard, N. *Proc. R. Soc. London, Ser. A* **1986**, *405*, 1.
(36) Jiang, L. Q.; Koel, B. E. *J. Phys. Chem. B* **1992**, *96*, 8694.
(37) Pick, S. *Surf. Sci.* **1999**, *436*, 220.
(38) Delbecq, F.; Sautet, P. *J. Catal.* **2003**, *220*, 115.
(39) Zhao, H.; Koel, B. E. *Surf. Sci.* **2004**, *572*, 261.
(40) Xu, C.; Koel, B. E. *Surf. Sci. Lett.* **1994**, *304*, L505.

JP903127B